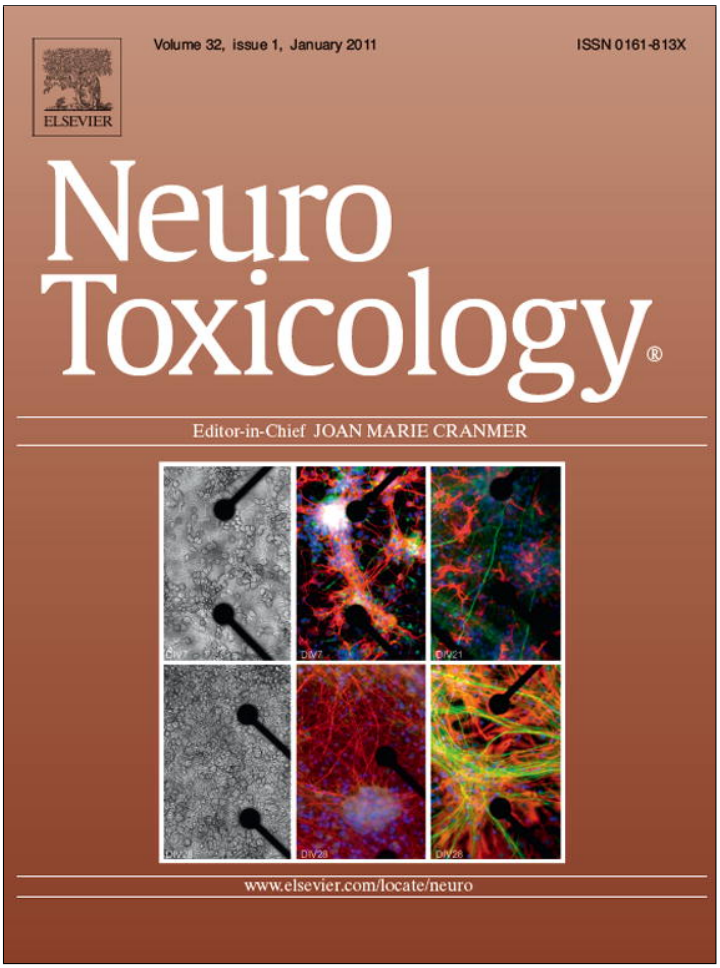

NeuroToxicology 32 (2011) 75–82

Contents lists available at ScienceDirect

NeuroToxicology

Iron overload triggers redox-sensitive signals in human IMR-32 neuroblastoma cells

Gabriela A. Salvador [a,*], Patricia I. Oteiza [b]

[a] Instituto de Investigaciones Bioquímicas de Bahía Blanca (INIBIBB), Consejo Nacional de Investigaciones Científicas y Técnicas (CONICET), Universidad Nacional del Sur, CC857, Camino La Carrindanga Km 7, B8000FWB Bahía Blanca, Buenos Aires, Argentina
[b] Departments of Nutrition and Environmental Toxicology, University of California, Davis, USA

ARTICLE INFO

Article history:
Received 29 October 2010
Accepted 25 November 2010
Available online 3 December 2010

Keywords:
Oxidative stress
Iron
Neurotoxicity
AP-1
NF-κB

ABSTRACT

Excessive neuronal iron has been proposed to contribute to the pathology of several neurodegenerative diseases including Alzheimer's and Parkinson's diseases. This work characterized human neuroblastoma IMR-32 cells exposure to ferric ammonium citrate (FAC) as a model of neuronal iron overload and neurodegeneration. The consequences of FAC treatment on neuronal oxidative stress and on the modulation of the oxidant-sensitive transcription factors AP-1 and NF-κB were investigated. Incubation with FAC (150 μM) resulted in a time (3–72 h)-dependent increase in cellular iron content, and was associated with cell oxidant increase. FAC caused a time-dependent (3–48 h) increase in nuclear AP-1- and NF-κB–DNA binding. This was associated with the upstream activation of the mitogen activated kinases ERK1/2, p38 and JNK and of IκBα phosphorylation and degradation. After 72 h incubation with FAC, cell viability was 40% lower than in controls. Iron overload caused apoptotic cell death. After 48–72 h of incubation with FAC, caspase 3 activity was increased, and chromatin condensation and nuclear fragmentation were observed. In summary, the exposure of IMR-32 cells to FAC is associated with increased oxidant cell levels, activation of redox-sensitive signals, and apoptosis.

1. Introduction

Over the past years, metallo-neurobiology has become extremely important for establishing the role of transition metals in neuronal degeneration. In this regard, high iron concentrations have been consistently observed in the brain of individuals with Alzheimer's disease (AD) and Parkinson's disease (Berg et al., 2001; Berg and Youdim, 2006). Iron progressively accumulates in the brain during normal aging, however, iron accumulation in AD occurs without the concomitant increase in ferritin normally observed with aging (Bartzokis et al., 2007; Connor et al., 1995; Quintana et al., 2006; Quintana and Gutierrez, 2010). In addition, a direct correlation between mutations in iron handling proteins and neurodegenerative processes has been demonstrated in a number of genetic neurodegenerative diseases such as ferritinopathy and Hallervorden–Spatz syndrome (Crompton et al., 2002).

The brain particularly needs iron for multiple physiological processes. Iron is a cofactor for tyrosine hydroxylase, tryptophan hydroxylase, xanthine oxidase and ribonucleoside reductase (Berg et al., 2001; Ke and Qian, 2007). Iron also participates in myelination, mitochondrial energy generation and DNA replication/cell cycling (Ortiz et al., 2004; Todorich et al., 2009). To maintain iron homeostasis, a series of iron-regulatory proteins exist for tightly control cellular iron uptake, storage, export and intracellular iron distribution (Ke and Qian, 2007; Kell, 2009). Whereas intracellular ferric iron is coupled to iron-storage proteins, free or weakly bound iron can participate in the Fenton reaction generating hydroxyl radicals. Hydroxyl radicals can damage membrane lipids, proteins and nucleic acids affecting neuronal function and causing cell death (Crichton and Charloteaux-Wauters, 1987; Halliwell, 2009). Thus, a tight neuronal iron balance is essential to meet the needs for several physiologic

Abbreviations: AD, Alzheimer's disease; ANOVA, analysis of variance; AP-1, activator protein-1; DCDHF, 5 (or 6)-carboxy-2′,7′-dichlorohydrofluorescein diacetate; DCF, 5-(and-6)-carboxy-2′,7′-dichlorofluorescein acid; DMEM, Dulbecco's modified Eagle medium; DTT, dithiothreitol; EDTA, ethylenediamine tetraacetate; EMSA, electrophoretic mobility shift assay; ERK1/2, extracellular signal-regulated kinase; FAC, ferric ammonium citrate; FBS, fetal bovine serum; HEPES, 4-(2-hydroxyethyl)-1-piperazineethanesulfonic; JNK, c-Jun-N-terminal kinase; MAPKs, mitogen activated protein kinases; NF-κB, nuclear factor-κB; OCT-1, octamer binding transcription factor-1; PAGE, polyacrylamide gel electrophoresis; PARP, poly (ADP-ribose) polymerase; PBS, phosphate-buffered saline; p-ERK, phosphorylated ERK; PI, propidium iodine; p-JNK, phosphorylated JNK; p-p38, phosphorylated p38; SDS, sodium dodecyl sulfate.

* Corresponding author. Tel.: +54 291 4861201; fax: +54 291 4861200.
E-mail address: salvador@criba.edu.ar (G.A. Salvador).

0161-813X/$ – see front matter © 2010 Elsevier Inc. All rights reserved.
doi:10.1016/j.neuro.2010.11.006

events, while avoiding the toxicity associated with iron overload (Ong and Farooqui, 2005; Salvador, 2010).

Neurons have developed several protective mechanisms against oxidative stress, one of them is the activation of signaling pathways that regulate the transcription of genes involved in antioxidant defenses and in repair mechanisms (Ahsan et al., 2009; Mackenzie et al., 2007; Mackenzie and Oteiza, 2007; Mattson, 2000; Mattson et al., 1998; Su et al., 2008; Uranga et al., 2009). The final neuronal response to an increase in oxidants will depend on the character, intensity and persistence of the oxidative insult (Saito et al., 2005). The characterization of the mechanisms mediating the adverse effects of iron on neuronal function and fate is central in understanding the pathophysiology of a number of neurodegenerative disorders.

This work characterized the sequence of oxidant-related events in a model of iron overload in neuronal cells. Human neuroblastoma IMR-32 cells were exposed to different concentrations of ferric ammonium citrate (FAC). FAC leads to a time-dependent iron accumulation that correlates with an increase in cellular oxidants. The activation of redox-sensitive signals increases up to 48 h after FAC exposure, at which point cellular apoptosis occurs. This model can be used to study the contribution of iron loading to the pathophysiology of neurodegenerative diseases.

2. Materials

IMR-32 cells were obtained from the American Type Culture Collection (Rockville, MA, USA). Cell culture media and reagents, were obtained from Invitrogen Life Technologies (Carlsbad, CA, USA). Antibodies for Erk (sc-93), p-Erk (sc-7383), JNK (sc-572), p-JNK (sc-6274) and PARP (sc-7150) were from Santa Cruz Biotechnology (Santa Cruz, CA, USA). Antibodies for p-IKBα (9246), and p-p38 (9211) were obtained from Cell Signaling Technology (Danvers, MA, USA). PVDF membranes were obtained from BIO-RAD (Hercules, CA, USA) and Chroma Spin-10 columns were from Clontech (Palo Alto, CA, USA). The ECL Western blotting system was from GE Healthcare (Piscataway, NJ, USA). The oligonucleotides containing the consensus sequence for NF-κB, AP-1 and OCT-1, the reagents for the EMSA, the CellTiter-Glo® Luminescent Cell Viability Assay, and 5 (or 6)-carboxy-2′,7′-dichlorohydrofluorescein diacetate (DCDCDHF) were obtained from Promega (Madison, WI, USA). FAC and all other reagents were from the highest quality available and were purchased from Sigma (St. Louis, MO, USA).

3. Methods

3.1. Cell culture

IMR-32 cells were cultured at 37°C, 5% (v/v) CO_2 in DMEM high glucose supplemented with 10% (v/v) fetal bovine serum (FBS) and antibiotics–antimicotic (50 U/mL penicillin, 50 μg/mL streptomycin and 0.125 μg/mL amphotericin B). IMR-32 cells were cultured in control medium up to 90% confluence. For the experiments, cells were incubated in DMEM high glucose with 5% (v/v) FBS for 3–72 h in the absence and presence of 50–150 μM FAC. The medium was changed every 2 days.

3.2. Determination of iron content

After 3–72 h of culturing IMR-32 cells in the absence or in the presence of 150 μM FAC, cells were collected for iron analysis. Cells (15×10^6) were rinsed twice with warm phosphate-buffered saline (PBS), scraped, and rinsed twice with PBS containing 1 mM desferoxamine. After the last centrifugation at 800 × *g* for 10 min at room temperature the pellet was frozen at −80 °C, and after thawing, resuspended in 0.4 mL of ultrapure water. After a brief sonication, an aliquot was taken for the determination of protein concentration and the rest of the sample was wet ashed with 16 M nitric acid (Baker's Instra-analyzed: J. T. Baker, Philipsburg, NJ, USA). Total cellular iron content was determined by ICP-AES (Trace Scan; Thermo Elemental, Franklin, MA, USA). Certified reference solutions (QC 21, Spec CentriPrep, Metuchen, NJ, USA) were used to generate the standard curve. A sample of a National Bureau of Standards Bovine Liver (SRM 1577; U.S. Department of Commerce, National Bureau of Standards, Washington, DC, USA) was included with the samples to ensure accuracy and reproducibility.

3.3. Cell viability assay

The effect of FAC on cell viability was determined using the CellTiter-Glo Luminescent Cell Viability Assay. Briefly, cells (60,000 cells/well) were incubated in the absence or in the presence of 50–150 μM FAC for different periods of time (0–72 h). Cell viability was measured following the procedures described by the manufacturer.

3.4. Determination of cell oxidant levels

Cell oxidant levels were evaluated using the probe DCDHF, which can cross the cell membrane, and after oxidation, is converted to 5-(and-6)-carboxy-2′,7′-dichlorofluorescein (DCDCDHF), a fluorescent compound. Cells (1×10^5) were grown in 12 well plates. After the corresponding treatments, the media was discarded; cells were rinsed with PBS and suspended in 200 μL of DMEM containing 15 μM DCDCDHF. After 1 h of incubation at 37 °C, the media was removed; cells were rinsed with PBS, and then incubated in 200 μL PBS containing 0.1% (v/v) Igepal. After 30 min of incubation with regular shaking, the fluorescence at 525 nm (λ_{exc}: 475 nm) was measured. To evaluate the DNA content, samples were subsequently incubated with 50 μM propidium iodide for 20 min at room temperature. The fluorescence (λ_{exc}: 538 nm, λ_{em}: 590 nm) was subsequently measured. Results are expressed as the ratio DCF/propidium iodide fluorescence.

3.5. Electrophoretic mobility shift assay (EMSA)

Nuclear cell fractions were prepared as previously described by Mackenzie et al. (2002, 2006). For the EMSA, the oligonucleotides containing the consensus sequence of NF-κB, and AP-1 were end labeled with [γ-32P] ATP using T4 polynucleotide kinase and purified using Chroma Spin-10 columns. Samples were incubated with the labeled oligonucleotide (20,000–30,000 cpm) for 20 min at room temperature in 1× binding buffer [5× binding buffer: 50 mM Tris–HCl buffer, pH 7.5, containing 20% (v/v) glycerol, 5 mM $MgCl_2$, 2.5 mM EDTA, 2.5 mM DTT, 250 mM NaCl and 0.25 mg/mL poly(dI–dC)]. The products were separated by electrophoresis in a 4–6% (w/v) non-denaturing polyacrylamide gel using 0.5×TBE (Tris/borate 45 mM, EDTA 1 mM) as the running buffer. The gels were dried and the radioactivity quantitated in a Phosphoimager 840 (Amersham Pharmacia Biotech. Inc., Piscataway, NJ, USA).

3.6. Western blot analysis

For the preparation of total cell extracts, cells (20×10^6 cells) were rinsed with PBS, scraped and centrifuged. The pellet was rinsed with PBS, and resuspended in 200 μL of 50 mM HEPES (pH 7.4), 125 mM KCl which contained protease inhibitors and 2% (v/v) Igepal. The final concentration of the inhibitors was 0.5 mmol/L PMSF, 1 mg/L leupeptin, 1 mg/L pepstatin, 1.5 mg/L aprotinin, 2 mg/L bestatin and 0.4 mM sodium pervanadate. Samples were

exposed to one cycle of freezing and thawing, incubated at 4 °C for 30 min and centrifuged at 15,000 × *g* for 30 min. The supernatant was decanted and protein concentration was measured (Bradford, 1976).

Aliquots of total cell lysates 25–50 μg protein were denatured with Laemmli buffer and were separated by reducing 10% (w/v) polyacrylamide gel electrophoresis and electroblotted to PVDF membranes. Colored molecular weight standards (Amersham, Piscataway, NJ, USA) were run simultaneously. Membranes were blotted for 2 h in 5% (w/v) non-fat milk, and subsequently incubated in the presence of corresponding primary antibodies (1:1000 dilution) overnight at 4 °C. After incubation for 90 min at room temperature in the presence of the secondary antibody (HRP-conjugated) (1:10,000 dilution) the conjugates were visualized by chemiluminescence detection in a Phosphoimager 840.

3.7. Hoechst staining

Cells (0.3×10^5) were plated onto L-polylysinated coverslips. After 72 h of incubation in the absence or presence of 150 μM FAC, the Hoechst reagent (10 μg/mL) was added to the media and incubated in the dark for 15 min at 37 °C. The media was subsequently discarded and cells were washed twice with PBS. Cells were fixed with 4% (w/v) paraformaldehyde in PBS for 15 min at room temperature, and after washing with PBS, coverslips were dried at room temperature. Finally, cells were mounted with Fluorsave and visualized by fluorescence microscopy (Olympus IMT-2).

3.8. Statistical analysis

One way analysis of variance (ANOVA) with subsequent post hoc comparisons by Scheffe, were performed using Statview 5.0.1 (Brainpower Inc., Calabazas CA, USA). A p value <0.05 was considered statistically significant. Values are given as mean ± SEM.

4. Results

4.1. FAC causes a time-dependent increase in IMR-32 cell iron content

To characterize the FAC-induced model of neuronal iron overload, we initially measured the kinetics of cellular iron accumulation. IMR-32 cells were incubated with 150 μM FAC for different periods (3–72 h) of time. Total cellular iron content, determined by ICP-AES, increased in a time-dependent manner. After 3 and 6 h incubation, cellular iron content was 1-fold and 3-fold higher, respectively, when compared to control (Fig. 1). After 24 h of FAC exposure, total iron content was 22-fold higher than control values and continued increasing up to 72 h (80-fold higher than control values) (Fig. 1).

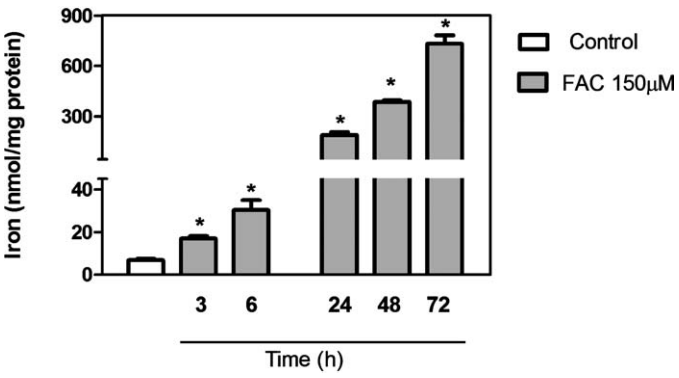

Fig. 1. FAC-induced iron overload in IMR-32 cells: IMR-32 cells were incubated for different periods of time (3–72 h) in the absence or in the presence of FAC (150 μM). Iron content was determined by ICP-AES as described under Sections 2 and 3. Results are shown as mean ± SEM of three independent experiments. *Significantly different compared to the respective control group ($p < 0.05$, one way ANOVA test).

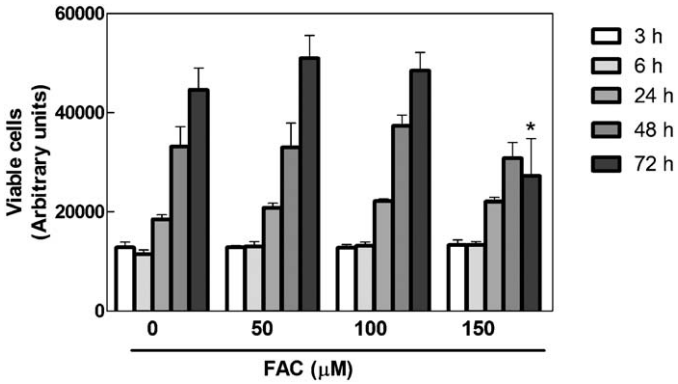

Fig. 2. Effect of FAC on IMR-32 cell viability: IMR-32 cells were incubated for different periods of time (3–72 h) in the absence or in the presence of FAC (50–150 μM). Cell viability was determined as described in Sections 2 and 3. Results are shown as mean ± SEM of three independent experiments. *Significantly different compared to values for cells incubated in the absence of FAC ($p < 0.05$, one way ANOVA test).

4.2. FAC-induced iron overload affects IMR-32 cell viability

Cell viability was assessed by measuring cellular ATP levels. IMR-32 cells were incubated in the presence of variable concentrations of FAC (50–150 μM) for different periods of time (3–72 h). At 50 μM and 100 μM, FAC did not affect cell viability at any of the times assayed (3–72 h). Cell viability was only affected (60% decrease compared to controls) at the highest FAC concentration (150 μM) and only after 72 h of incubation (Fig. 2).

4.3. FAC-induced iron overload increases oxidant levels in IMR-32 cells

We next evaluated if FAC-induced iron accumulation could cause an increase in cell oxidants. For this purpose, IMR-32 cells were incubated in the presence of variable concentrations of FAC (50–150 μM) for different periods of time (3–72 h) and cell

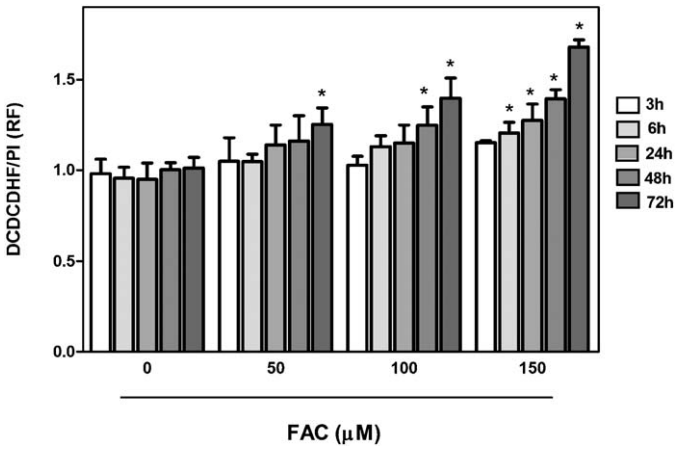

Fig. 3. FAC increases cell oxidant levels in IMR-32 cells: IMR-32 cells were incubated for different periods of time (3–72 h) in the absence or in the presence of FAC (50–150 μM). Cell oxidants were measured with the probe DCDHF as described under Sections 2 and 3. Fluorescence was corrected by the DNA content measured with propidium iodine (PI). Results are shown as mean ± SEM of three independent experiments. *Significantly different compared to values for cells incubated in the absence of FAC ($p < 0.05$, one way ANOVA test).

oxidant levels were measured with the probe DCDHF. The fluorescence of the oxidized probe (DCF) was corrected by the DNA content measured with propidium iodide (PI). In cells exposed to 50 μM FAC, the increase in cell oxidants iodide was significant only after 72 h of incubation. At 100 μM FAC, oxidants were significantly higher after 48 and 72 h of incubation (22% and 38%, respectively). At 150 μM FAC, cell oxidants levels were already significantly higher after 6 h of incubation, and continued increasing in a time-dependent manner up to 72 h (Fig. 3). A significant correlation ($r^2 = 0.99$, $p < 0.05$) was found between cellular iron content and cell oxidant levels.

4.4. FAC-induced iron overload activates mitogen activated kinases (MAPKs) in IMR-32 cells

The MAPKs ERK1/2, p38 and JNK are known to be activated by several pro-oxidant stressors such as H_2O_2, Pb^{2+}, and Fe^{2+} (Aimo and Oteiza, 2006; Davila and Torres-Aleman, 2008; Kim and Wong,

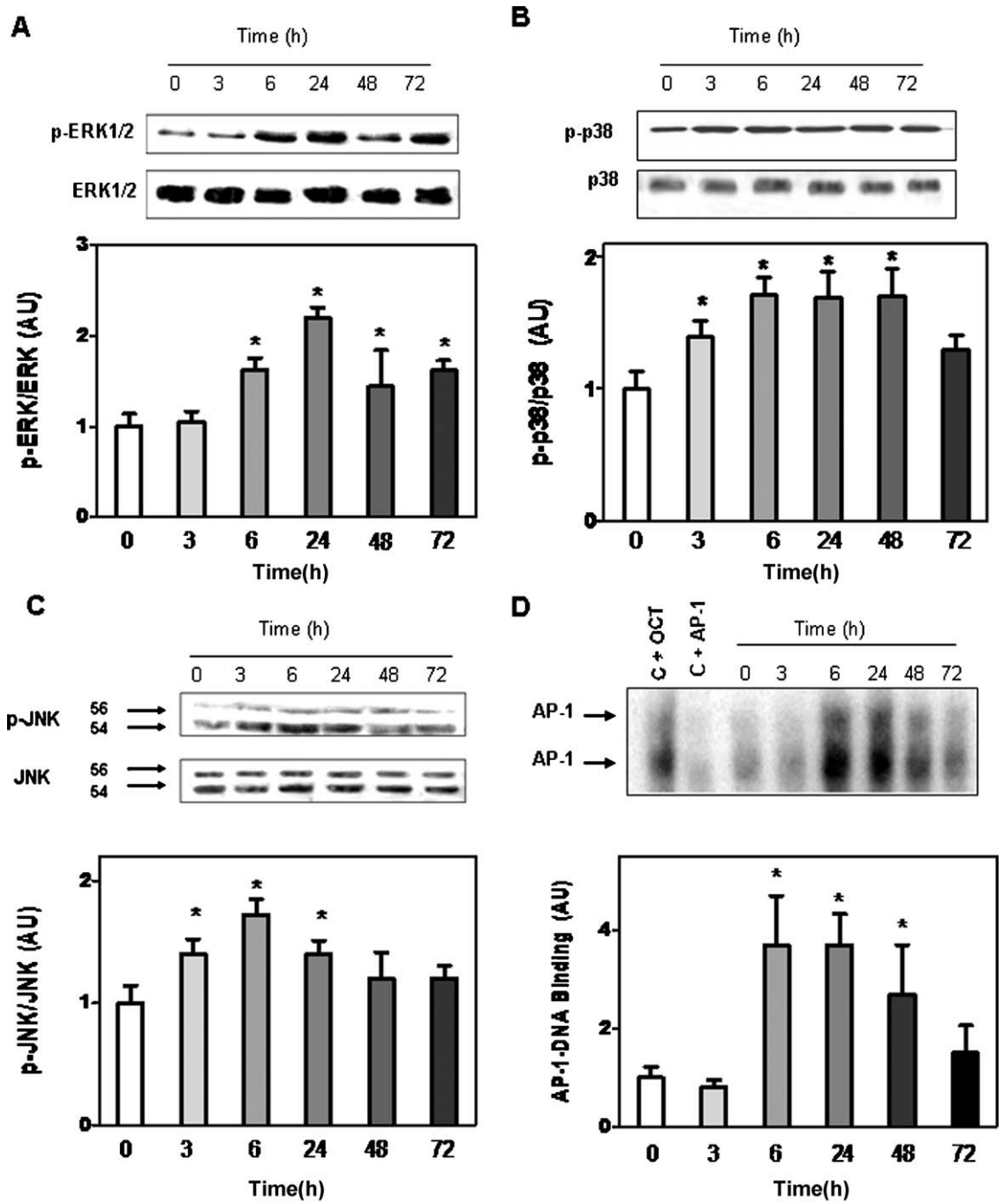

Fig. 4. FAC causes MAPK and AP-1 activation: IMR-32 cells were incubated for different periods of time (3–72 h) in the absence or in the presence of FAC (150 μM). Western blots in total cell fractions for (A) phosphorylated ERK1/2 (p-ERK1/2) and ERK1/2; (B) phosphorylated p38 (p-p38) and p38; and (C) phosphorylated JNK (p-JNK) and JNK. After quantitation, the ratios phosphorylated/non-phosphorylated protein levels were calculated and results are shown as mean ± SEM of three independent experiments. (D) The activation of transcription factor AP-1 was evaluated by measuring the AP-1–DNA binding activity in nuclear fractions by EMSA. The specificity of the AP-1–DNA bands was determined by competition with a 100-fold molar excess of unlabeled oligonucleotide containing the consensus sequence for either AP-1 or OCT-1. A representative EMSA image is shown. After quantitation, results are shown as mean ± SEM of three independent experiments. *Significantly different compared to values for cells incubated in the absence of FAC ($p < 0.05$, one way ANOVA test).

2009; Uranga et al., 2009). We next investigated the possible activation of these MAPKs by iron overload. IMR-32 cells were incubated in the absence or presence of 150 μM FAC for different periods of time (3–72 h), and the levels of ERK1/2, p38, and JNK phosphorylation were evaluated by Western blot. ERK1/2 phosphorylation levels increased significantly after 6 h of incubation with 150 μM FAC, reaching maximum levels (100% increase) after 24 h of incubation. ERK1/2 phosphorylation levels remained high up to 72 h of incubation (Fig. 4A). In the presence of 100 μM FAC ERK 1/2 activation showed a similar profile (data not shown).

An increase in p38 phosphorylation was evident after 3 h of incubation with 150 μM FAC, and remained high up to 48 h of incubation (Fig. 4B). The increase in JNK phosphorylation was significant after 3 h of incubation with 150 μM FAC, peaked at 6 h (72% higher than controls) and returned to basal levels after 48 and 72 h of incubation with FAC (Fig. 4C).

ERK1/2, p38 and JNK are known to be upstream activators of AP-1 activation. AP-1 activation was assessed by measuring the AP-1–DNA binding in nuclear cell fractions by EMSA. The specificity of the AP-1–DNA bands was determined by competition with a 100-fold molar excess of unlabeled oligonucleotide containing the consensus sequence for either AP-1 or OCT-1 (Fig. 4D). FAC caused a time-dependent increase in AP-1–DNA-binding. It was significant after 6 h (270%) of incubation, remained elevated until 48 h of incubation (170%), and reached basal levels at 72 h (Fig. 4D). Similar results were observed after cell incubation with 100 μM FAC (data not shown).

4.5. FAC-induced iron overload activates transcription factor NF-κB in IMR-32 cells

Oxidative stress can also trigger activation of the transcription factor NF-κB (Dhandapani et al., 2005; Mackenzie et al., 2002; Meffert et al., 2003). The phosphorylation and degradation of the inhibitory protein IκB is one of the required steps for NF-κB activation (Fig. 5A). FAC-induced increase in NF-κB binding followed a similar pattern to that of AP-1. It peaked after 6 h (75% higher than $t = 0$) of incubation with FAC and remained high up to 24 h of incubation (Fig. 5B). In accordance with the EMSA results, the increased levels of IκBα phosphorylation, and the decreased levels of the inhibitor IκB content parallels with the increased nuclear NF-κB–DNA binding.

4.6. FAC-induced iron overload promotes apoptotic cell death

We next evaluated if, similarly to that observed in neurodegeneration, FAC could induce apoptosis. One of the defining features of apoptotic cell death is the activation of caspases. Particularly, caspase 3 activation constitutes an irreversible step in the apoptotic cascade. Compared to control conditions, caspase 3 activity was increased by 200 and 300% in cells incubated with 150 μM FAC for 48 and 72 h, respectively (Fig. 6A). PARP is a substrate of caspase 3, which catalyzes its cleavage from a full length protein (116 kDa) to a 85 kDa fragment. In agreement with the caspase 3 activity data, PARP cleavage was significantly higher (43% and 62%), in cells exposed to 150 μM FAC for 48 and 72 h, respectively (Fig. 6B).

Apoptotic changes upon 150 μM FAC exposure were evaluated by phase-contrast microscopy and nuclear staining with the DNA dye Hoechst 33258. After 72 h of FAC exposure cell morphology was overtly affected, displaying evident morphological alterations including rounded cell body with a decreased number of cell projections (Fig. 6C). Moreover, nuclear morphology evaluated by Hoechst staining showed typical apoptotic changes; chromatin condensation and nuclear fragmentation (Fig. 6D).

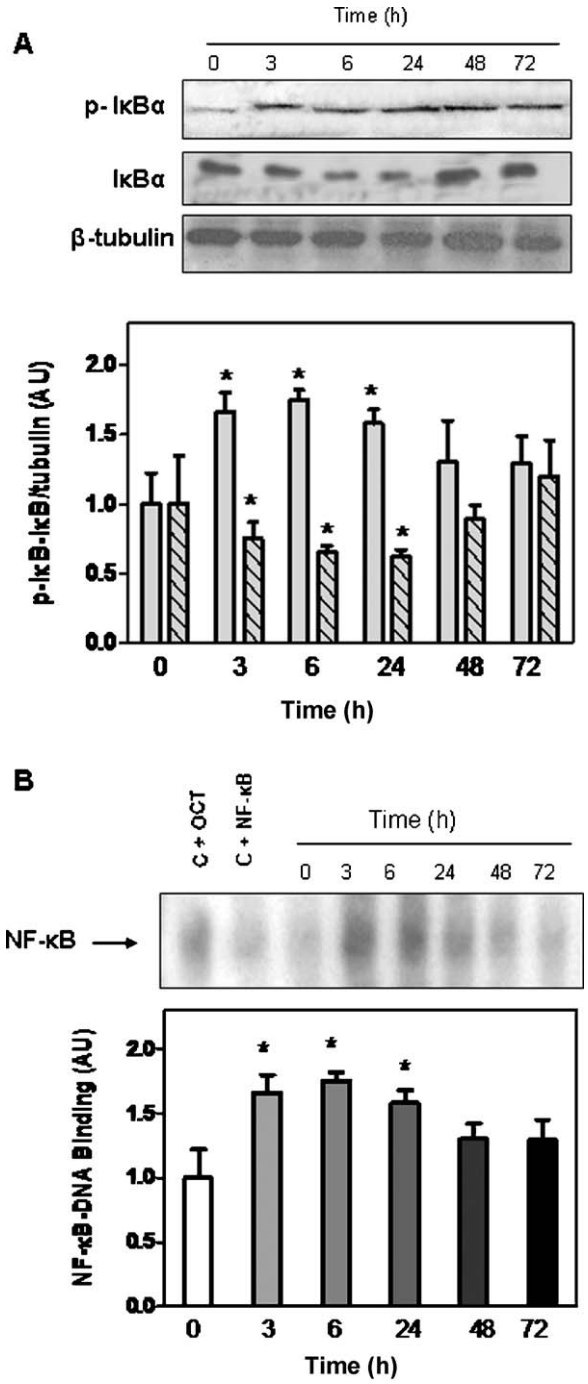

Fig. 5. FAC causes NF-κB activation in IMR-32 cells: IMR-32 cells were incubated for different periods of time (3–72 h) in the absence or in the presence of FAC (150 μM). (A) Western blots in total cell fractions for phosphorylated IκBα (p-IκBα), IκBα and β-tubulin. One representative Western blot image is shown after quantitation, p-IκBα (solid bars) and IκBα (stripped bars) levels were referred to the β-tubulin content. (B) The activation of transcription factor NF-κB was evaluated by measuring NF-κB–DNA binding in nuclear fractions by EMSA. The specificity of the NF-κB–DNA bands was determined by competition with a 100-fold molar excess of unlabeled oligonucleotide containing the consensus sequence for either NF-κB or OCT-1. One representative EMSA image is shown. After quantitation results are shown as mean ± SEM of three independent experiments. *Significantly different compared to values for cells incubated in the absence of FAC ($p < 0.05$, one way ANOVA test).

5. Discussion

Neurons are particularly susceptible to oxidative stress and they have developed several protective mechanisms that involve a direct alteration in transcription factors and their upstream

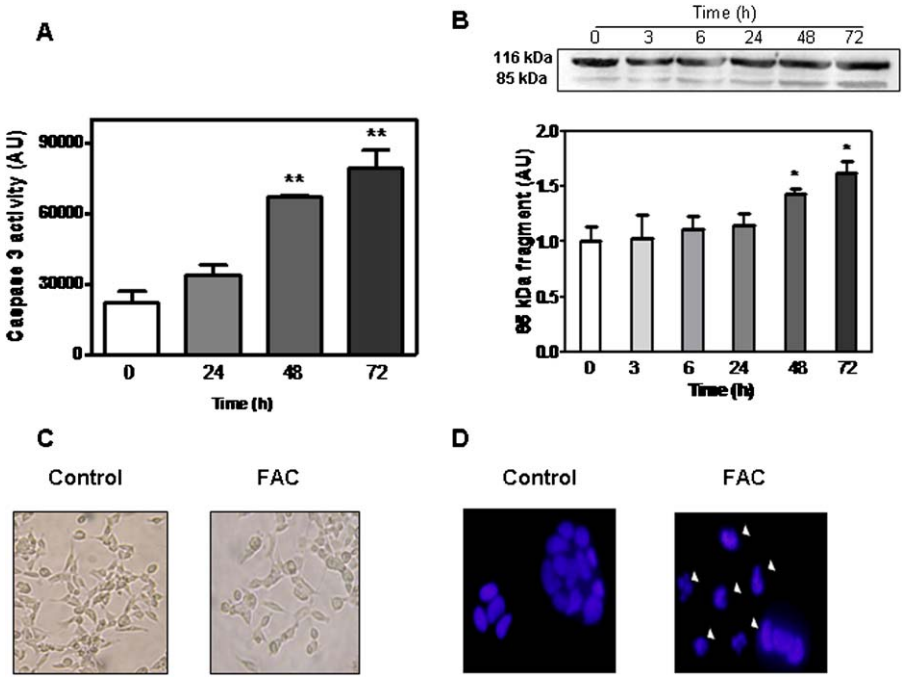

Fig. 6. FAC induces apoptosis in IMR-32 cells: IMR-32 cells were incubated for different periods of time (24–72 h) in the absence or in the presence of FAC (150 μM) (A) Caspase-3 activity was measured as indicated in Sections 2 and 3. (B) PARP fragmentation was evaluated by Western blot. One representative Western blot image of three independent experiments is shown. For A and B results are shown as mean ± SEM of three independent experiments. Significantly different compared to values from cells incubated in the absence of FAC ($p < 0.05$, one way ANOVA test). (C) Phase contrast microscopy of neuroblastoma IMR-32 cells after the incubation of IMR-32 cells for 72 h in the absence or in the presence of FAC (150 μM). (D) Nuclei staining with Hoechst evaluated by fluorescence microscopy. White spots indicate nuclear fragmentation and chromatin condensation.

kinases for counteracting the deleterious effects of oxidative injury (Ahsan et al., 2009; Andersen, 2004; Davila and Torres-Aleman, 2008). Upon oxidative stress, neuronal death or survival will depend on the balance between the activation of pro-oxidant and anti-oxidant signaling. Thus, knowledge of the cross-talk between iron-induced neurotoxicity and redox signaling is critical to understand the molecular mechanisms that operate in neurodegenerative disorders (Barnham and Bush, 2008; Berg and Youdim, 2006). In our model of progressive iron overload we show that iron accumulation causes an increase in cell oxidants, which trigger the early activation of redox-sensitive signaling cascades (MAPKs, AP-1 and NF-κB).

Human neuroblastoma IMR-32 cells incubated in the presence of FAC accumulate iron, and show an increase in the steady state levels of cellular oxidants in a time- and concentration-dependent manner. The association of cell iron accumulation and increased oxidant production is supported by the strong correlation between both parameters. Similar FAC concentrations were used in a model of macular degeneration using retinal pigment epithelium cells (Volobоueva et al., 2007). In these studies, cell exposure to increasing FAC concentrations also resulted in a time- and dose dependent rise in intracellular iron, with concomitant increased oxidant production and decreased glutathione levels and mitochondrial complex IV activity (Volobоueva et al., 2007).The same extent of iron accumulation in neurons exposed to FAC was reported by Bishop et al. (2010). In our experiments, we did not detect a significant increase in oxidant levels up to 24–48 h of iron exposure despite the progressive increase in iron levels. This late increase in cellular oxidants support the concept that neuronal cells have developed tightly regulated protective mechanisms for buffering the pool size of labile iron. In this regard, the expression of ferritin and transferrin receptors is regulated by iron regulatory proteins (IRP1 and IRP2), which in turn are regulated by non-chelated and redox active iron (Crichton and Charloteaux-Wauters, 1987; Ke and Qian, 2007; Kell, 2009). This tight regulation of iron homeostasis is altered in AD, mainly due to the elevated iron levels complexed with ferritin observed in the vicinity of amyloid plaques and the strong affinity of β amyloid peptide for iron, which are 8 orders of magnitude stronger than that of transferrin (Barnham and Bush, 2008; Jiang et al., 2009).

Cell viability was only affected at the highest concentration of FAC assayed (150 μM) and after 72 h of incubation in spite of the progressive increase in cellular iron content observed at 24 and 48 h. This high resistance to iron-mediated toxicity induced by FAC incubation was also observed in primary cultured neurons (Bishop et al., 2010). This could be due to the up-regulation of redox-sensitive signaling pathways which promote transcriptional activation of a set of genes involved in antioxidant protection and repair mechanisms.

It is well known that the MAPKs ERK1/2, p38 and JNK are sensitive to conditions that cause oxidative stress including metal neurotoxicity (Aimo and Oteiza, 2006; Kuperstein and Yavin, 2002, 2003; Uranga et al., 2009). Accordingly, we found that ERK1/2, p38 and JNK are activated by FAC exposure following a similar pattern of phosphorylation, increasing up to 24 h and subsequently returning to basal levels. ERK1/2 activation is involved both in neuronal survival and in cellular death (Fan et al., 2007). Several *in vitro* and *in vivo* studies showed that alterations of JNK pathways are associated with neuronal death in Parkinson's and Alzheimer's diseases (Borsello and Forloni, 2007). JNK and p38 are also involved in anti-apoptotic signaling (Brown and Benchimol, 2006; Ikeda et al., 2008). This dual role of MAPKs opens interesting questions about their specific role in neurotoxicity processes.

One of the upstream regulated targets of MAPK activation is transcription factor AP-1 (Mossman et al., 2006). This transcription factor regulates multiple processes including cell proliferation, differentiation, survival and apoptosis (Ogunwobi and Beales, 2007). Upon FAC exposure AP-1 activation occurred in the same

time frame that ERK1/2, p38 and JNK activation. The protective function of AP-1 has been related through the regulation of the expression of heme-oxygenase-1 and Mn-superoxide dismutase (Mn-SOD), which in turn are important for the development of oxidant tolerance (Morse et al., 2003; Rui and Kvietys, 2005).

Prior to the appearance of apoptotic evidence, the oxidant sensitive transcription factor NF-κB was activated by FAC-induced iron overload. NF-κB was the first eukaryotic transcription factor described as responsive to the cellular redox state. Specifically in neurons, NF-κB can be activated by a variety of signals including oxidants, and the amyloid precursor protein (in its secreted form) (Mattson et al., 1998; Meffert et al., 2003). The anti-apoptotic action of NF-κB in neurons has been proposed to be related through the regulation of the expression of Bcl-2, SOD, cyclin D-1 and Bcl-xl (Mattson, 2000; Meffert et al., 2003; Ogunwobi and Beales, 2007). NF-κB activation is also involved in the protection of cerebellar granular cells against oxidative insults generated by an increase in free iron levels (Kaltschmidt et al., 2002). This protection against iron-induced oxidative injury could be due to the increased transcription of the ferritin H chain and also to the expression of anti-apoptotic genes (Kwak et al., 1995). In view of the results presented here, the activation of NF-κB during iron overload could constitute a mechanism of protection and of increasing the neuronal capacity to buffer labile iron pools. Moreover, the long-lasting activation (24–48 h) of AP-1 and NF-κB strongly suggest a key function for these transcription factors in neuronal iron overload as that observed in neurodegenerative processes. The concerted action of NF-κB and AP-1 was involved in the development of oxidant tolerance in cardiac myocytes (Rui and Kvietys, 2005).

In conclusion, this work shows that the exposure of human neuroblastoma IMR-32 cells to FAC results in iron accumulation, increased production of oxidants and the activation of redox-sensitive signals. This experimental approach of progressive neuronal iron overload can be a useful model to study the sequence of oxidant-related events in iron-associated neurodegeneration. However, further studies are needed to confirm these initial observations in order to ascertain the precise role of MAPK, AP-1 and NF-κB signaling as neuroprotective or pro-apoptotic during iron-induced neurotoxicity.

Conflict of interest

The authors declare that there are no conflicts of interest.

Acknowledgments

This study was supported by the Agencia Nacional de Promoción Científica y Tecnológica (ANPCYT), the Consejo Nacional de Investigaciones Científicas y Técnicas (CONICET, Argentina) and the University of California (Davis). GAS is a research member of the CONICET, and she was a Postdoctoral Fulbright Fellow in the Department of Nutrition, University of California, Davis. PIO is a Correspondent Researcher from the CONICET.

References

Ahsan MK, Lekli I, Ray D, Yodoi J, Das DK. Redox regulation of cell survival by the thioredoxin superfamily: an implication of redox gene therapy in the heart. Antioxid Redox Signal 2009;11:2741–58.

Aimo L, Oteiza PI. Zinc deficiency increases the susceptibility of human neuroblastoma cells to lead-induced activator protein-1 activation. Toxicol Sci 2006;91:184–91.

Andersen JK. Oxidative stress in neurodegeneration: cause or consequence? Nat Med 2004;10(Suppl.):S18–25.

Barnham KJ, Bush AI. Metals in Alzheimer's and Parkinson's diseases. Curr Opin Chem Biol 2008;12:222–8.

Bartzokis G, Tishler TA, Lu PH, Villablanca P, Altshuler LL, Carter M, et al. Brain ferritin iron may influence age- and gender-related risks of neurodegeneration. Neurobiol Aging 2007;28:414–23.

Berg D, Gerlach M, Youdim MB, Double KL, Zecca L, Riederer P, et al. Brain iron pathways and their relevance to Parkinson's disease. J Neurochem 2001;79:225–36.

Berg D, Youdim MB. Role of iron in neurodegenerative disorders. Top Magn Reson Imaging 2006;17:5–17.

Bishop GM, Dang TN, Dringen R, Robinson SR. Accumulation of non-transferrin-bound iron by neurons, astrocytes, and microglia. Neurotox Res 2010.

Borsello T, Forloni G. JNK signalling: a possible target to prevent neurodegeneration. Curr Pharm Des 2007;13:1875–86.

Bradford MM. A rapid and sensitive method for the quantitation of microgram quantities of protein utilizing the principle of protein-dye binding. Anal Biochem 1976;72:248–54.

Brown L, Benchimol S. The involvement of MAPK signaling pathways in determining the cellular response to p53 activation: cell cycle arrest or apoptosis. J Biol Chem 2006;281:3832–40.

Connor JR, Snyder BS, Arosio P, Loeffler DA, LeWitt P. A quantitative analysis of isoferritins in select regions of aged, parkinsonian, and Alzheimer's diseased brains. J Neurochem 1995;65:717–24.

Crichton RR, Charloteaux-Wauters M. Iron transport and storage. Eur J Biochem 1987;164:485–506.

Crompton DE, Chinnery PF, Fey C, Curtis AR, Morris CM, Kierstan J, et al. Neuroferritinopathy: a window on the role of iron in neurodegeneration. Blood Cells Mol Dis 2002;29:522–31.

Davila D, Torres-Aleman I. Neuronal death by oxidative stress involves activation of FOXO3 through a two-arm pathway that activates stress kinases and attenuates insulin-like growth factor I signaling. Mol Biol Cell 2008;19:2014–25.

Dhandapani KM, Wade FM, Wakade C, Mahesh VB, Brann DW. Neuroprotection by stem cell factor in rat cortical neurons involves AKT and NFkappaB. J Neurochem 2005;95:9–19.

Fan Y, Chen H, Qiao B, Luo L, Ma H, Li H, et al. Opposing effects of ERK and p38 MAP kinases on HeLa cell apoptosis induced by dipyrithione. Mol Cells 2007;23:30–8.

Halliwell B. The wanderings of a free radical. Free Radic Biol Med 2009;46:531–42.

Ikeda F, Matsubara T, Tsurukai T, Hata K, Nishimura R, Yoneda T. JNK/c-Jun signaling mediates an anti-apoptotic effect of RANKL in osteoclasts. J Bone Miner Res 2008;23:907–14.

Jiang D, Li X, Williams R, Patel S, Men L, Wang Y, et al. Ternary complexes of iron, amyloid-beta, and nitrilotriacetic acid: binding affinities, redox properties, and relevance to iron-induced oxidative stress in Alzheimer's disease. Biochemistry 2009;48:7939–47.

Kaltschmidt B, Heinrich M, Kaltschmidt C. Stimulus-dependent activation of NF-kappaB specifies apoptosis or neuroprotection in cerebellar granule cells. Neuromolecular Med 2002;2:299–309.

Ke Y, Qian ZM. Brain iron metabolism: neurobiology and neurochemistry. Prog Neurobiol 2007;83:149–73.

Kell DB. Iron behaving badly: inappropriate iron chelation as a major contributor to the aetiology of vascular and other progressive inflammatory and degenerative diseases. BMC Med Genomics 2009;2:2.

Kim J, Wong PK. Loss of ATM impairs proliferation of neural stem cells through oxidative stress-mediated p38 MAPK signaling. Stem Cells 2009;27:1987–98.

Kuperstein F, Yavin E. ERK activation and nuclear translocation in amyloid-beta peptide- and iron-stressed neuronal cell cultures. Eur J Neurosci 2002;16:44–54.

Kuperstein F, Yavin E. Pro-apoptotic signaling in neuronal cells following iron and amyloid beta peptide neurotoxicity. J Neurochem 2003;86:114–25.

Kwak EL, Larochelle DA, Beaumont C, Torti SV, Torti FM. Role for NF-kappa B in the regulation of ferritin H by tumor necrosis factor-alpha. J Biol Chem 1995;270:15285–93.

Mackenzie GG, Oteiza PI. Zinc and the cytoskeleton in the neuronal modulation of transcription factor NFAT. J Cell Physiol 2007;210:246–56.

Mackenzie GG, Zago MP, Aimo L, Oteiza PI. Zinc deficiency in neuronal biology. IUBMB Life 2007;59:299–307.

Mackenzie GG, Zago MP, Erlejman AG, Aimo L, Keen CL, Oteiza PI. Alpha-lipoic acid and N-acetyl cysteine prevent zinc deficiency-induced activation of NF-kappaB and AP-1 transcription factors in human neuroblastoma IMR-32 cells. Free Radic Res 2006;40:75–84.

Mackenzie GG, Zago MP, Keen CL, Oteiza PI. Low intracellular zinc impairs the translocation of activated NF-kappa B to the nuclei in human neuroblastoma IMR-32 cells. J Biol Chem 2002;277:34610–7.

Mattson MP. Apoptotic and anti-apoptotic synaptic signaling mechanisms. Brain Pathol 2000;10:300–12.

Mattson MP, Keller JN, Begley JG. Evidence for synaptic apoptosis. Exp Neurol 1998;153:35–48.

Meffert MK, Chang JM, Wiltgen BJ, Fanselow MS, Baltimore D. NF-kappa B functions in synaptic signaling and behavior. Nat Neurosci 2003;6:1072–8.

Morse D, Pischke SE, Zhou Z, Davis RJ, Flavell RA, Loop T, et al. Suppression of inflammatory cytokine production by carbon monoxide involves the JNK pathway and AP-1. J Biol Chem 2003;278:36993–8.

Mossman BT, Lounsbury KM, Reddy SP. Oxidants and signaling by mitogen-activated protein kinases in lung epithelium. Am J Respir Cell Mol Biol 2006;34:666–9.

Ogunwobi OO, Beales IL. The anti-apoptotic and growth stimulatory actions of leptin in human colon cancer cells involves activation of JNK mitogen activated protein kinase, JAK2 and PI3 kinase/Akt. Int J Colorectal Dis 2007;22:401–9.

Ong WY, Farooqui AA. Iron, neuroinflammation, and Alzheimer's disease. J Alzheimers Dis 2005;8:183–200.

Ortiz E, Pasquini JM, Thompson K, Felt B, Butkus G, Beard J, et al. Effect of manipulation of iron storage, transport, or availability on myelin composition and brain iron content in three different animal models. J Neurosci Res 2004;77:681–9.

Quintana C, Bellefqih S, Laval JY, Guerquin-Kern JL, Wu TD, Avila J, et al. Study of the localization of iron, ferritin, and hemosiderin in Alzheimer's disease hippocampus by analytical microscopy at the subcellular level. J Struct Biol 2006;153:42–54.
Quintana C, Gutierrez L. Could a dysfunction of ferritin be a determinant factor in the aetiology of some neurodegenerative diseases? Biochim Biophys Acta 2010.
Rui T, Kvietys PR. NFkappaB and AP-1 differentially contribute to the induction of Mn-SOD and eNOS during the development of oxidant tolerance. FASEB J 2005;19: 1908–10.
Saito A, Maier CM, Narasimhan P, Nishi T, Song YS, Yu F, et al. Oxidative stress and neuronal death/survival signaling in cerebral ischemia. Mol Neurobiol 2005;31: 105–16.
Salvador GA. Iron in neuronal function and dysfunction. Biofactors 2010;36:103–10.
Su B, Wang X, Nunomura A, Moreira PI, Lee HG, Perry G, et al. Oxidative stress signaling in Alzheimer's disease. Curr Alzheimer Res 2008;5:525–32.
Todorich B, Pasquini JM, Garcia CI, Paez PM, Connor JR. Oligodendrocytes and myelination: the role of iron. Glia 2009;57:467–78.
Uranga RM, Giusto NM, Salvador GA. Iron-induced oxidative injury differentially regulates PI3K/Akt/GSK3beta pathway in synaptic endings from adult and aged rats. Toxicol Sci 2009;111:331–44.
Voloboueva LA, Killilea DW, Atamna H, Ames BN. N-tert-butyl hydroxylamine, a mitochondrial antioxidant, protects human retinal pigment epithelial cells from iron overload: relevance to macular degeneration. FASEB J 2007;21:4077–86.